SUBMICROSECOND SHOCK-INDUCED CHEMICAL REACTIONS IN SOLIDS: FIRST REAL-TIME OBSERVATIONS ☆

M.B. BOSLOUGH and R.A. GRAHAM

Sandia National Laboratories, Albuquerque, NM 87185, USA

Received 6 June 1985; in final form 30 August 1985

We report observations of a chemical reaction on a 100 ns time scale in a nickel–aluminum powder mixture while under high-pressure shock loading. Optical pyrometer measurements show values of spectral radiance that can only be explained by high temperatures due to an exothermic reaction. Streak photography shows spatial evolution of the reaction zone in regions of the sample predicted to experience shock pressures and temperatures known to initiate formation of nickel–aluminum alloys.

1. Introduction

Chemical effects in condensed matter subjected to high-pressure shock compression have recently become the object of considerable fundamental study [1]. This interest is stimulated by the potential of the shock process to create new or significantly modified materials and by the potential for chemical observations to improve understanding of the shock process [2]. Examination of samples after shock loading has shown that chemical changes are readily induced by the shock event. Nevertheless, the shock-compression process is complex, and quantitative, fundamental study requires knowledge of conditions at which chemical reactions are initiated and the conditions under which the reaction proceeds. Thus, one of the most compelling issues in shock chemistry is the need to identify particular features of the shock process with chemical effects. Does chemistry occur during the risetime of the loading pulse, during the relatively quiescent shock-compressed state, during pressure release or in the post-shock heated state?

In recent work, Horie and co-workers [3] have shown from post-shock analysis of samples that mechanically mixed powders of nickel and aluminum react to form nickel aluminides when shock-induced temperatures are greater than about 500°C. In similar work the reaction of nickel–aluminum composite powders is found to lead to products different from those of the mechanically mixed powders [4]. Titanium aluminides are also formed under similar conditions [5].

The present paper provides direct evidence for the initiation of strong chemical reaction in mechanically mixed powders of aluminum and nickel in the shock-compressed state. The reaction is observed to initiate within 100 ns after shock conditioning of particles in the early part of the pressure pulse and application of critical values of pressure and temperature. This evidence is based on observations from experiments which use optical pyrometry and streak photography to measure spectral and spatial time histories of the light output from the shocked powder compacts. The experiments are supported by appropriate computer simulation [6] of the shock process.

2. Experimental

Powder compacts were pressed in place in experimental fixtures to densities of 4.25 Mg/m^3 (about 60% of solid density). Aluminum and nickel powders were mechanically blended to nominal compositions of 30 vol % Al and 70 vol % Ni. The powders were

☆ This work was performed at Sandia National Laboratories supported by the US Department of Energy under contract No. DE-AC04-76DP00789.

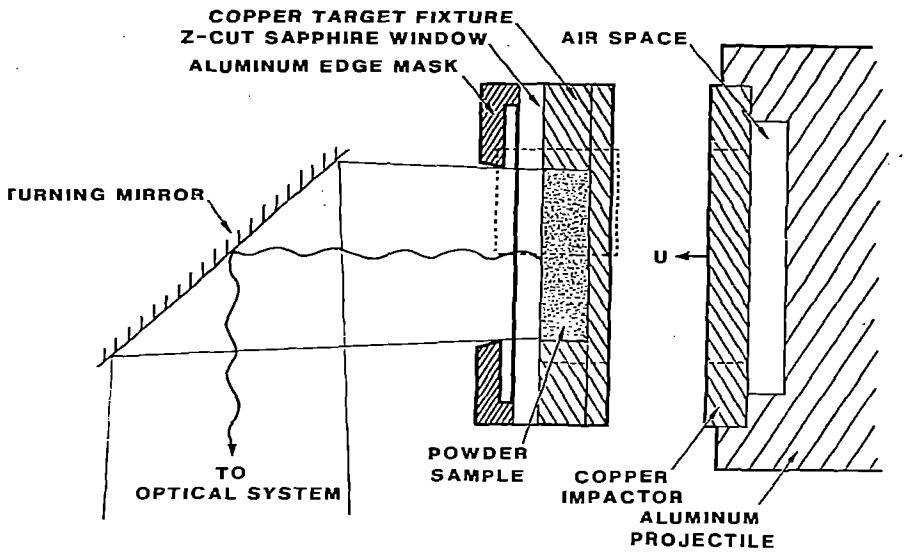

Fig. 1. The experimental configuration which involves the precise controlled impact of a copper plate on a copper sample holder at a velocity of 1 km/s. Light radiated from the powder–sapphire interface due to the shock compression is reflected into one of two different optical systems. The rectangle with lightly dotted borders outlines the area displayed in fig. 2.

CERAC A-1189 aluminum and CERAC N-1095 nickel. Nominal particle sizes were 5 to 15 μm and 44 to 74 μm, respectively. The alumimum was of nominal 99.99% purity while the nickel was of 99.9% nominal purity.

The experimental fixtures for the samples were designed for precise shock loading in impact experiments with a 63 mm diameter compressed gas gun [7]. Copper capsules with radial guard rings were impacted with copper impactors with similar guard rings at nominal velocities of 1 km/s. At this impact velocity the impact stress in the copper is 21 GPa before two-dimensional effects are experienced. As indicated in fig. 1, the surface of the powder compact opposite the impact plane is pressed against a *Z*-cut sapphire plate which acts as an optical port to view the powder. The sapphire is known to have a Hugoniot elastic limit of up to 20 GPa under shock loading [8]. Light from the powder sample is radiated through the sapphire (which remains transparent under shock) and reflected from a local turning mirror into the optical instrumentation.

Two types of instrumentation were used in separate experiments. An optical pyrometer which measures absolute light intensity (spectral radiance) is calibrated at four different wavelengths and observes the radiance from the entire 25.4 mm aperture of the target fixture. The four wavelengths are 0.5, 0.9, 1.4 and 1.8 μm with bandwidths of about 0.2 μm. The risetimes of the 0.5 and 0.9 μm detectors are about 12 ns and the 1.4 and 1.8 μm detector risetimes are about 20 ns. The four signals were simultaneously digitized at a 200 MHz sampling rate (5 ns interval). The system is similar to that described by Boslough [9].

The second system consists of an Imacon 500 image converter streak camera with an image intensifier system. The aperture of the target is imaged onto a slit, which collects light from only a narrow strip about 1 mm wide and 25.4 mm (the diameter of the sample) long. This image is swept across the film at a rate of about 1 μs/cm to produce a streak record containing both spatial and temporal information in the visible. In this experiment a fraction of the light was split off and sent to two photomultiplier tubes from which an uncalibrated total light intensity history was recorded. More detail on similar streak measurements with this instrumentation is described by Setchell [10].

In typical real-time shock compression experiments

the loading is arranged to provide a large region in which the conditions are maintained in a state of one-dimensional strain. For this situation conventional shock wave conservation relations can be applied to obtain pressures and temperatures in the samples. For the present case in which low-density powder compacts are placed in metal containers, a wave trapping phenomenon occurs such that the principal part of the loading history is dominated by two-dimensional effects [6,11]. Moreover, the pressure and temperature required to initiate the chemical reaction in recovery experiments was found by Horie and co-workers to be dominated by the two-dimensional effects. In the present experiments, one-dimensional, initial shock conditions would not lead to pressures and temperatures sufficiently high to initiate the reaction and we anticipated that two-dimensional effects would dominate.

3. Results

Evidence for an exothermic reaction occurring while the powder is still under high pressure stems from: (1) the high intensity of light measured by the pyrometer, (2) the spatial pattern of emission measured by streak photography in the hot outer region predicted by the two-dimensional numerical calculations, (3) the correspondence between shock conditions in the hot outer region to those of the prior work of Horie and co-workers which showed formation of new chemical products.

Interpretation of the time dependence of the light emission and the conditions under which reaction occurs as well as correlation with prior explosive-loading post shock analysis requires detailed study of shock conditions with a two-dimensional computer code. The Sandia CSQ computer code is used with a model powder material based on shock compression data of rutile powder [6,11,12]. The output of the numerical simulation of sample response is a detailed temporal and spatial history of two-dimensional pressure and mean bulk temperature. Numerous computer experiments have determined that the principal factor governing the response is the relatively low density of the powder compact compared to the copper sample holder. As indicated in fig. 2, which shows contours of temperature through one half of the cross section of the sample at various times, the thermal response is dominated by rapid propagation of the stress pulse through the copper on the outer edge of the powder. This situation caused the powder in the outer edge to be loaded due to compression moving through the powder and also moving radially inward from the copper. As shown in fig. 2b, the multidimensional loading causes a hot region to develop. In the numerical simulation this hot region propagates toward the powder–sapphire interface and impinges on that interface at 2.7 μs after impact, the time at which pressure release from the sapphire free surface reduces the pressure to 17 GPa. As time progresses, the pressure and high-temperature region propagates radially inward. At 3.4 μs after impact the longitudinal wave moving along the axis arrives at the sapphire–powder interface and the pressure at the interface reaches 13 GPa with a temperature of about 650°C.

The pyrometer records (fig. 3) show that immediately upon arrival of the shock wave through the higher-impedance copper to the copper–sapphire interface (see fig. 2, axial position 14 mm, radial position >13 mm), a low-level light emission is observed at the shorter wavelengths (starting at time A, fig. 3). There are two possible sources for this low-level radiation: (1) highly localized hot regions which are the result of inhomogeneous deposition of deformation energy [2,13,14] so that a small fraction of the shocked material reaches a temperature much higher than the mean bulk temperature (only about 450°C) predicted by the numerical simulation, (2) low-level, non-thermal radiation from the shocked sapphire by unknown mechanisms similar to that observed by Brooks, Brannon and others for quartz and lithium niobate [15–17].

The low-level light emission level remains fairly constant until the first shock wave reflects from the sapphire free surface and returns at approximately 2.7 μs after impact (time B in fig. 3) as a reduction of pressure at the sapphire–powder interface (see fig. 2, axial position 14 mm, radial position <13 mm). The spectral radiance at all wavelengths increases suddenly, as observed over the entire face of the sample, within 200 ns of time B. At a wavelength of 500 nm, the spectral radiance reaches 1.6×10^{11} W sr^{-1} m^{-3}, characteristic of blackbody temperatures of nearly 3000 K. The true temperature is significantly higher as the streak record shows that the light is radiating from only a fraction of the total sample area at

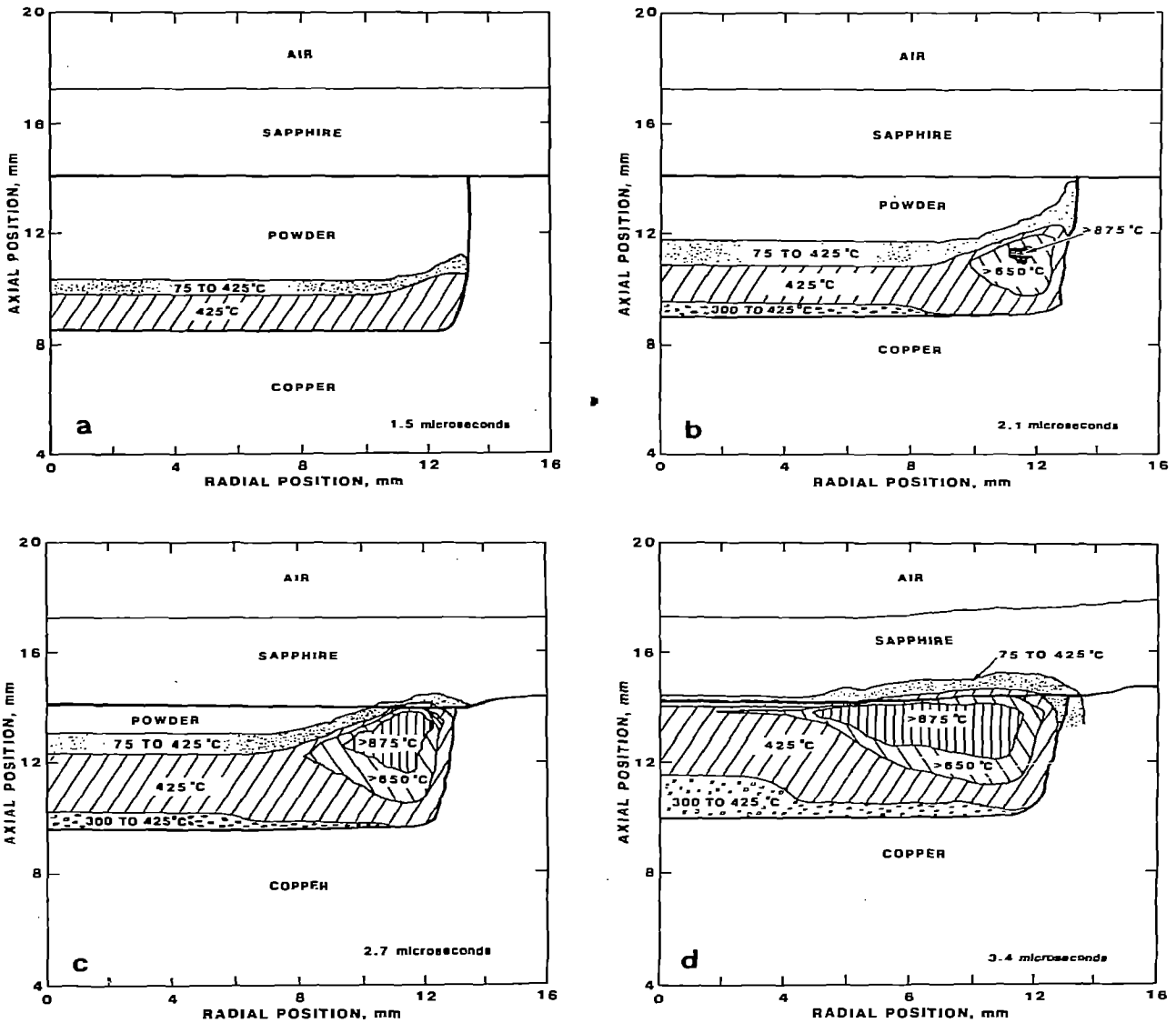

Fig.2. Results of two-dimensional numerical calculations, giving mean bulk temperatures of shocked material at various times after impact. (a) $t = 1.5$ μs: sapphire is undisturbed. (b) $t = 2.1$ μs: shock has arrived at copper–sapphire interface. Edge effects have generated a hot zone in the powder, but it is not visible through the sapphire window. (c) $t = 2.7$ μs: material sufficiently hot for the reaction to occur has arrived at the powder–sapphire interface where it can be viewed by the instrumentation. (d) $t = 3.4$ μs: the amount of hot material visible at the interface has greatly increased. The direct (longitudinal) shock has arrived at the interface near the axis.

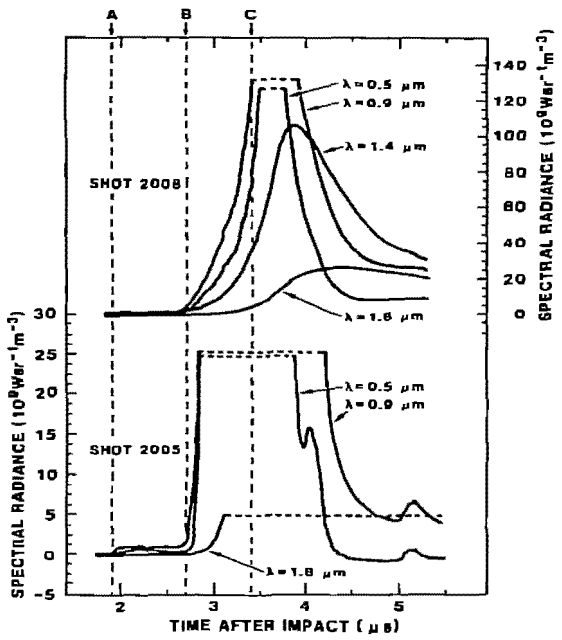

Fig. 3. Time-resolved light output at several wavelengths for two experiments. Impact time is derived from triggering time of shot 2005, and was inferred for shot 2008 which triggered early. Off scale signal is denoted by dashed lines. Marked times (as determined from simulation) are A: shock arrival at copper–sapphire interface, B: arrival of hot region at powder–sapphire interface, and C: arrival of direct (longitudinal) shock at powder sapphire interface. Note that the scale is more sensitive for shot 2005.

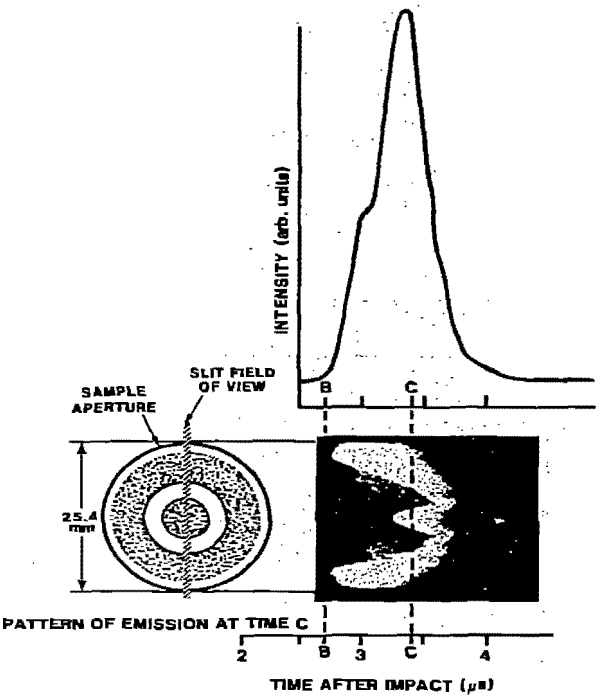

Fig. 4. Streak record from shot 2026 shows a converging reaction zone. The relative aperature size is shown in the lower left, with a superimposed slit field of view (hatched). The photomultiplier tube record is shown above the streak record with approximately the same time scaling. Times marked B and C are the same as those in fig. 3. The approximate pattern of emission at time C is shown in the lower left.

any given time, and the spectral emissivity of the radiating material is likely to be much less than unity. A two-parameter least-squares fit to the pyrometer data gives a peak temperature of 5000 K with an effective emissivity of about 0.01. The effective emissivity includes the absolute material emissivity and a reduction factor equal to the fraction of the surface which is radiating.

The streak camera record shown in fig. 4 shows intense light emission which begins at the same time as the pyrometer record. The source of the light is initially limited to the outer region of the sample where the numerical simulation predicts temperatures greater than 500°C, the value found in the prior work [3–5] to be required to initiate the reaction leading to formation of intermetallic alloys. This observation of the light emission from the same location that the numerical simulation determined to be sufficiently hot for ignition is clear evidence that the light is associated with an exothermic reaction. The streak camera is insensitive to temperatures of around 500°C. Only an exothermic reaction could increase the temperature sufficiently for the thermal radiation to be observable by the camera as a bright streak.

As the streak proceeds in time from left to right, the record shows a radial spreading of the reaction outward as well as inward from its initial position at time B in fig. 4. At any given point in the sample, the strong emission of light lasts only about 1/2 μs and then rapidly diminishes. This reduction of light occurs at the proper time to correspond to the adiabatic cooling due to the reduction of pressure by unloading

from the free surface. The pyrometer data show that the material is still radiating strongly in the near infrared after the bright flash of visible light is no longer detectable by the streak camera; hence, the residual temperature remains high.

The streak camera record shows the beginning of an intense reaction along the axis of the sample about 500 ns after the reaction is initiated in the outer regions of the sample. Upon first examination this new reaction appears to be due to radial loading waves converging on the axis. However, this behavior is not consistent with the numerical simulation which shows radial convergence on the axis to arrive several hundred nanoseconds after the observed axial reaction. It is possible that the numerical simulations do not provide a realistic description of the radial convergence due to an inadequate description of the aluminum–nickel powder shock compression behavior. This point requires further study.

It is also possible that the onset of the axial reaction is a reflection of the pressure dependence of the initiation of reaction. The numerical simulation shows that initiation of reaction in the outer region of the sample occurs at a pressure of about 17 GPa and temperature of greater than 500°C. The high-temperature region is predicted to move radially inward more rapidly than the observed radial movement of the light emission in the streak camera record. The numerical simulation predicts the arrival of the direct compression wave along the axis at the sapphire–powder interface at the time the axial reaction is observed. The peak pressure at that time is 15 GPa. At intermediate radial locations along the sapphire–powder interface the pressures are significantly greater than on the axis, ranging from 30 to 40 GPa. The behavior predicted by the numerical simulation is consistent with a situation in which pressure in excess of about 20 GPa prevents the initiation of reaction even though the temperature is in excess of 500°C. Although this latter point is consistent with all observation and numerical simulations, a model in which pressure inhibits the initiation requires much more extensive study before it can be accepted.

4. Conclusions

The present work provides the first direct evidence for shock-induced chemical reactions in solids on the submicrosecond time scale. Chemical reaction on this time scale requires an extraordinarily enhanced solid-state reactivity which the conditions accompanying shock compression provide: surfaces are cleaned, new surfaces are created, highly defective structural states are achieved, localized mass motion is mechanically forced, large local gradients of temperature and pressure are produced and crystallite sizes are modified. These conditions can reasonably be expected to greatly accelerate chemical processes. Although the existence of chemical reactions due to shock loading has been known for many years, explicit evidence for the existence of submicrosecond chemical reactions in solids under high pressure demonstrates the uniquess of the shock process. Such fast chemical reactions may lead to synthesis of new materials and synthesis of existing materials with significantly different properties. The existence of fast chemical reactions also requires that considerable care be given to the interpretation of shock compression processes on the basis of physical effects alone.

Acknowledgement

The authors are pleased to acknowledge discussions with Y. Horie, D.M. Webb, W.J. Hammetter and R.E. Setchell and the technical assistance of M.U. Anderson, K. Elsner and D.E. Wackerbarth.

References

[1] B. Morosin and R.A. Graham, in: Shock waves in condensed matter 1981, Menlo Park, eds. W.J. Nellis, L. Seaman and R.A. Graham (Am. Inst. Phys., New York, 1982) pp. 4–13.
[2] G.E. Duvall, Shock compression chemistry in materials synthesis and processing, National Academy of Sciences, National Research Council, National Materials Advisory Broad, Publication NMAB-414 (National Academy Press, Washington, 1984).
[3] Y. Horie, R.A. Graham and I.K. Simonsen, Mat. Letters 3 (1985) 354.
[4] H.R. Pak, Y. Horie and R.A. Graham, American Physical Society, 1985 Topical Conference on Shock Waves in Condensed Matter, Spokane, WA (July 20–25, 1985).
[5] D.E.P. Hoy, Y. Horie and R.A. Graham, American Physical Society, 1985 Topical Conference on Shock Waves in Condensed Matter, Spokane, WA (July 20–25, 1985).

[6] R.A. Graham and D.M. Webb, in: Shock waves in condensed matter 1983, eds. J.R. Asay, R.A. Graham and G.K. Straub (North-Holland, Amsterdam, 1985) pp. 211–214.
[7] R.E. Setchell, in: Shock waves in condensed matter 1981, Menlo Park, eds. W.J. Nellis, L. Seaman and R.A. Graham (Am. Inst. Phys., New York, 1982) p. 657.
[8] R.A. Graham and W.P. Brooks, J. Phys. Chem. Solids 32 (1971) 2311.
[9] M.B. Boslough, Ph.D. thesis, California Institute of Technology, Pasadena (1983).
[10] R.E. Setchell, in: The Eighth Symposium (International) on Detonation, Albuquerque (July 15–19, 1985).
[11] L. Davison, D. Webb and R.A. Grahm, in: Shock waves in condensed matter 1981, Menlo Park, eds. W.J. Nellis, L. Seaman and R.A. Graham (Am. Inst. Phys., New York, 1982).
[12] R.A. Graham and D.M. Webb, in: American Physical Society, 1985, Topical Conference on Shock Waves in Condensed Matter, Spokane, WA (July 20–25, 1985).
[13] K. Kondo and T.J. Ahrens, Phys. Chem. Minerals 9 (1983) 173.
[14] D.R. Schmitt and T.J. Ahrens, Geophys. Res. Letters 10 (1983) 1077.
[15] W.P. Brooks, J. Appl. Phys. 36 (1965) 2788.
[16] P.J. Brannon, C. Konrad, R.W. Morris, E.D. Jones and J.R. Asay, J. Appl. Phys. 54 (1983) 6374.
[17] P.J. Brannon, R.W. Morris and J.R. Asay, J. Appl. Phys. 57 (1985) 1676.